2006

Structure and Vibrational Spectra of Mononitrated Benzo [a] Pyrenes.

Kefa Karimu Onchoke
Stephen F Austin State University, onchokekk@sfasu.edu

Christopher M. Hadad

Prabir K. Dutta

Structure and Vibrational Spectra of Mononitrated Benzo[*a*]pyrenes

Kefa K. Onchoke, Christopher M. Hadad, and Prabir K. Dutta*

Department of Chemistry, The Ohio State University, 100 W. 18th Avenue, Columbus, Ohio 43210

Received: August 29, 2005; In Final Form: October 17, 2005

The molecules benzo[*a*]pyrene (BaP) and 1-, 3-, and 6-nitrobenzo[*a*]pyrene (1-NBaP, 3-NBaP, 6-NBaP) are currently of significant interest due to their presence in respirable combustion exhaust particulates and their mutagenic and carcinogenic properties. Structure−function correlations as well as spectroscopic signatures for trace analysis are necessary for these benzo[*a*]pyrene derivatives. In this paper, detailed infrared and Raman spectroscopic data of BaP and its three mononitrated isomers are provided for the first time. By utilizing density functional theory (DFT, B3LYP method with 6-311+G** basis set), the molecular geometries and the vibrational spectra are calculated. Good agreement is noted between the calculated and experimental geometry for BaP, and predictions of the vibrational data for all compounds are within ∼5 cm^{-1} of the experimental data. Normal mode assignments are proposed with particular emphasis on the nitro group vibrations. The geometrical distortions of the BaP structure upon nitro group substitution and correlations between structural parameters and vibrational data as well as structure−function relationships related to the mutagenicity of this important class of polycyclic aromatic hydrocarbons are discussed.

Introduction

Nitro-substituted polycyclic aromatic hydrocarbons (NPAHs) are members of a class of environmental contaminants found in airborne particulate matter, fossil fuel combustion products, coal fly ash, cigarette smoke, and vehicular emissions, formed by reactions of polycyclic aromatic hydrocarbons (PAHs) with nitrogen oxides.[1−5] Because of their mutagenic, carcinogenic, tumorigenic, and teratogenic activities, NPAHs pose significant health threats to humans.[2,5−8] Typically, NPAHs can be 100 000 times more mutagenic and 10 times more carcinogenic as compared to the unsubstituted parent PAHs.

Past investigations[9−14] have employed gas-phase, matrix-assisted isolation methods (together with theoretical methods) to provide infrared (IR) spectroscopic and structural signatures of PAHs. For benzo[*a*]pyrene and its derivatives, detailed spectroscopic data are lacking. Such data are necessary for developing trace analysis of these compounds by sensitive vibrational spectroscopic techniques, such as surface enhanced spectroscopies. Also, the significant differences in the mutagenic properties between the various BaP nitro isomers (1- and 3- are more toxic than the 6-isomer) are related to their structure and correlations between vibrational spectra and biological activities can have predictive powers for toxicity of nitro-PAHs. While the Raman and IR spectra of BaP have been studied,[15−20] its comprehensive normal-mode analysis is unavailable. For NPAHs,[21,22] there are very few IR/Raman studies and even fewer normal-mode analyses. Carrasco et al.[23,24] investigated the spectra of 2-nitrofluorene and 1-nitropyrene and have made normal mode assignments on the basis of both experimental and theoretical studies. For NBaPs, there are only two studies. Li et al.[8] made assignments of 6-nitrobenzo[*a*]pyrene (6-NBaP) on the basis of group frequency tables. Dyker et al..[25] reported the synthesis of 1- and 3-nitrobenzo[*a*]pyrene (1-NBaP, 3-NBaP) and, as part of their analytical characterization, reported the frequencies of a few of the major infrared bands.

Because comprehensive experimental and theoretical studies of the important monosubstituted NBaPs are lacking, this study was undertaken with the following objectives:

(a) to obtain IR and Raman spectra of 1-, 3-, and 6-NBaP;

(b) to perform DFT (B3LYP, 6-311+G**) calculations on BaP and 1-, 3-, and 6-NBaP to obtain geometrical data and the corresponding vibrational frequencies;

(c) to assign all experimental frequencies using normal-mode analysis.

On the basis of these experimental and theoretical data, we correlate the geometrical changes in the BaP structural motif with substitution of the nitro group at the different positions. Trends in the vibrational frequencies, especially those relating to the nitro group in the three isomers, are discussed. Finally, possible relationships between the structure of NBaPs and their biological activity are described.

Experimental Methods

Caution! *All compounds in this study are known carcinogens and mutagens. Therefore all necessary safety precautions were taken in handling them.*

Synthesis. All chemical reagents were of analytical grade and were purchased from Sigma-Aldrich (Milwaukee, WI). Benzo[*a*]pyrene was passed through a silica gel (200−430 mesh) column and cleaned up with hexane. NMR analytical grade solvents were purchased from Aldrich Chemical Co. (Milwaukee, WI). The 1-, 3-, and 6-nitrobenzo[*a*]pyrene (1-, 3-, and 6-NBaP) were synthesized by known published procedures.[6,26,27] The separation of 1- and 3-NBaP (with very close dipole moments, calculated as 6.4 and 6.5 D, respectively) was achieved via medium-pressure liquid chromatography (MPLC). The ^{1}H NMR chemical shifts in ppm, downfield from internal tetramethylsilane (TMS), and UV−vis spectra were confirmed in agreement with literature reports.[28] ^{1}H NMR (500 MHz, $CDCl_3$, δ): (a) 1-NBaP, 9.30−9.28 (d, H-11), 9.19−9.21 (d, H-12), 9.08−9.11 (d, H-10), 8.73−8.75 (d, H-3), 8.68 (s, H-6), 8.34−8.36 (d, H-7), 8.19−8.21 (d, H-5), 8.09−8.11 (d, H-2),

* Corresponding author. E-mail: Dutta.1@osu.edu. Fax: 614-688-5402.

10.1021/jp054881d CCC: $33.50
Published on Web 12/07/2005

7.96−7.98 (d, H-4), 7.94−7.97 (m, H-9), 7.87−7.90 (t, H-8); (b) 3-NBaP, 9.20−9.23 (d, H-11), 9.05−9.06 (d, H-10), 8.72−8.74 (d, H-4), 8.64 (s, H-6), 8.57−8.59 (d, H-1), 8.34−8.35 (d, H-12), 8.32−8.36 (t, H-7), 8.23−8.25 (d, H-5), 8.20−8.22 (d, H-2), 7.92−7.95 (t, H-9), 7.85−7.88 (t, H-8); (c) 6-NBaP, 9.09−9.11 (m, H-10), 9.05−9.07 (d, H-11), 8.44−8.46 (d, 12), 8.36−8.37 (d, H-1), 8.21−8.23 (d, H-3), 8.18−8.20 (m, H-7), 8.12−8.14 (d, H-5), 8.07−8.10 (t, H-2), 7.95−7.93 (m, H-4), 7.90−7.92 (m, H-8 and H-9). ^{13}C NMR ($CDCl_3$, 125.74 MHz, δ): 1-NBaP, 143.01, 136.46, 135.21, 131.76 (C-5), 131.55, 129.18 (C-7), 129.03, 128.78, 128.23 (C-6), 127.43 (C-9), 127.01 (C-8), 126.97 (C-4), 125.93, 125.90 (C-11), 124.65, 123.68 (C-3), 123.51 (C-2), 123.16 (C-10), 122.80, 122.22 (C-12); 3-NBaP, 142.87, 134.27, 132.58 (C-5), 131.53, 129.31, 129.24, 128.22, 127.65, 127.34 (C-9), 126.93 (C-8), 125.90, 125.47, 125.18, 125.03 (C-2), 123.12, 123.10 (C-10), 122.25 (C-1), 121.63 (C-4); 6-NBaP, 132.57, 131.14 (C-5), 130.30, 129.87 (C-12), 129.09, 128.32 (C-9), 127.83, 127.68 (C-1), 127.04 (C-8), 126.97 (C-2), 126.94 (C-3), 124.52, 123.30 (C-10), 122.34 (C-7), 122.32, 122.29, 121.86 (C-11), 121.84, 121.12, 120.57 (C-4). ^{13}C NMR assignments were made based on HMQC experiments.

Instrumentation. Solution and solid FT infrared spectra were recorded on a Perkin-Elmer 16PC spectrometer equipped with deuterated triglycine sulfate (DTGS) detector. Solid FT-IR spectra were recorded on KBr (99% FT-IR grade, Aldrich) pellet at a resolution of 4 cm^{-1} in the 4000−450 cm^{-1} region. A total of 1000 scans or more were collected in the transmission mode. Solution FT-IR spectra were recorded in CCl_4 with two KBr windows for IR transmission down to 450 cm^{-1} with a 0.1 mm spacer. Raman spectra were recorded on a FT-Raman spectrometer on a Bruker model FRA-106 attachment, connected to an equinox 55 IR system with a quartz beam splitter. Radiation of 1064 nm from an ND:YAG Adlas laser was used for excitation at a power of 60−120 mW. The solid samples were placed in a brass holder. A total of 1000 or more scans were accumulated at a resolution of 4 cm^{-1}. Data acquisition was performed using Bruker OPUS software (version 4). A Blackman-Harris 3-term apodization function was used. Solution FT-Raman spectra were recorded in methylene chloride and chloroform. UV−vis spectra was recorded with a Shimadzu 2501PC spectrophotometer from 200 to 550 nm and confirmed to be in agreement with reports in the literature.[6,7,28]

Computational Details

All of the DFT calculations were performed with the GAUSSIAN 98 package[29] of programs at the Ohio Supercomputer Center. The geometries of all structures were fully optimized at the Becke three-parameter[30,31] hybrid exchange functional combined with the Lee−Yang−Parr[32] correlation functional, with the standard 6-31G*[33] and 6-311+G** basis sets. In all computations, no constraints were imposed on the geometry. Full geometry optimization was performed until a stationary point for the local minima was found. All optimized geometries were confirmed to be stationary points or minima by a vibrational frequency calculation. The normal modes and vibrational frequencies were evaluated at the computed equilibrium geometries by analytic evaluation of energy second derivatives based on the harmonic approximation. Scaling factors of 0.9614[34] and 0.98[35] were used for vibrational frequencies at the B3LYP/6-31G* and B3LYP/6-311+G** levels, respectively.[36] Because of the large numbers of fundamental frequencies, the assignments of bands were made on the basis of potential energy distribution (PED) calculations by transforming the normal coordinate displacements from the Cartesian to an internal coordinate basis using the NMODES[37] program. Normal mode animations were made possible with the programs Molecule 1.3.5 and MOLEKEL 4.3.[38] Vibrational assignments of the experimental frequencies in this study are based upon (i) PEDs calculations derived from the B3LYP/6-311+G** level of theory, (ii) the description of the motions and comparisons of calculated and observed FT-Raman and FT-IR, and (iii) visual inspection of the eigenvectors for each mode. Optimized Cartesian coordinates, complete structural parameters, vibrational frequencies, and assignments are available in the Supporting Information (Tables S1−S13).

Results

Assessment of Computational Methodology. To provide confidence in the calculations, the geometry of nitrobenzene and BaP was calculated using both 6-31G* and 6-311+G** and compared to available experimental data.[39−42] Structural parameters for nitrobenzene on the basis of electron and microwave diffraction data have been reported, and single-crystal X-ray diffraction on BaP has been performed. Figure 1 represents the numbering scheme of optimized structures of nitrobenzene, BaP, and 1-, 3-, and 6-NBaP used in the text. Using bond lengths (C−C, C−N, N−O), bond angles (C−C−C, O−N−O, C−C−N), and C−C−C−C and C−C−N−O dihedral angles, comparisons between experimental structural data and calculations were made (Table 1). We note good agreement between calculated and available experimental data,[39] especially with the calculations done with the 6-311+G** basis set. For example, in nitrobenzene, the N−O bond distance is 1.2272/1.2234 Å[41] and the calculated value is 1.2245 Å. For BaP, the two shortest bonds are at C13−C14 and C8−C9 as observed from X-ray diffraction data[39] and are also predicted by the calculations. All of the subsequent sections will be focused on structural and vibrational data derived at the B3LYP/6311+G** level of theory.

Structures of the NBaPs. Though X-ray structural data are available for 6-NBaP,[43] no such data are available for 1- and 3-NBaP. Selected optimized structural parameters of BaP, 1-, 3-, and 6-NBaP are presented in Tables 2 and 3, while the complete data set for BaP and the three nitro isomers is available in Supporting Information Tables S6−S9.

1-Nitrobenzo[*a*]pyrene (1-NBaP). Upon substitution of the nitro group in the 1-position, the shortest bonds still remain in the same part of the molecule (C8−C9, C13−C14 in BaP and C21−C22, C31−C32 in 1-NBaP), as shown in Table 2. The C−N bond length is predicted as 1.4722 Å, and the N−O bond lengths are 1.2283 and 1.2276 Å. The ring is essentially planar, with largest C−C−C−C dihedral angle for C6−C5−C32−C31 of 1.4° and N2−C4−C5−C32 with a dihedral angle of 3°. Dihedral angles between the aromatic ring and atoms O1−N2−C4−C5 and O3−N2−C4−C25 were calculated as 29 and 27°, respectively (Table 2).

3-Nitrobenzo[*a*]pyrene (3-NBaP). The shortest bond lengths in 3-NBaP (C21−C22, C26−C27) are also located in the same position as in BaP. The C−N bond length is predicted to be 1.4732 Å, slightly longer than the 1-NBaP, and the N−O bond length is 1.2280 and 1.2275 Å, almost comparable to 3-NBaP. The ring is essentially planar, with the largest C−C−C−C dihedral angles for C22−C5−C6−C7 and C5−C4−C30−C29 predicted as 1.7 and 1.8°, respectively, and the N2−C4−C5−C22 with a dihedral angle of 2.7°. The C−H bond lengths change very little, as compared to BaP. The dihedral angles between the aromatic ring and the nitro group, i.e., O1−N2−C4−C5 and O3−N2−C4−C30, are calculated as 30.5 and 28.8°, respectively (Table 2).

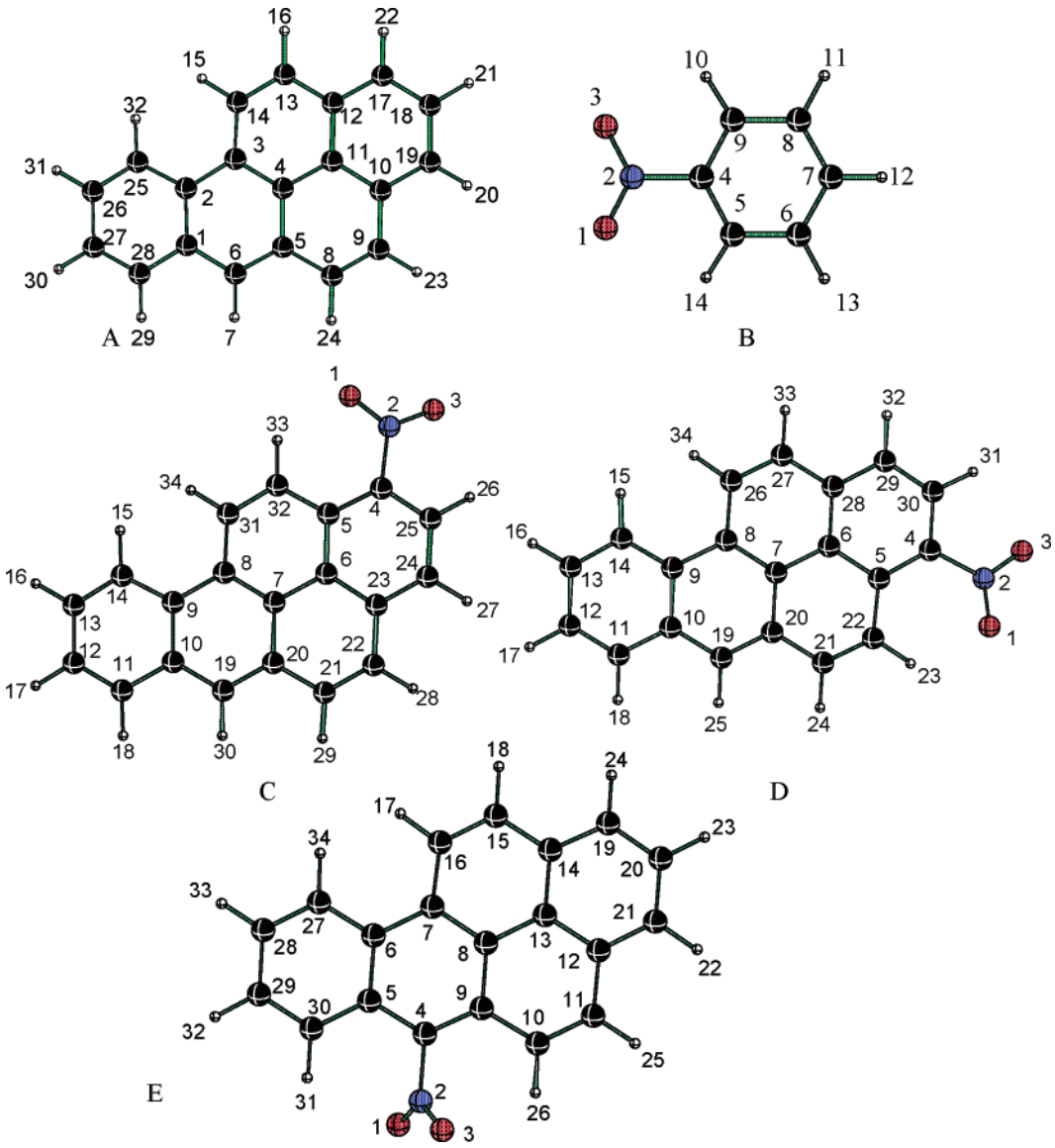

Figure 1. Numbering system of optimized structures: (A) benzo[*a*]pyrene; (B) nitrobenzene; (C) 1-nitrobenzo[*a*]pyrene; (D) 3-nitrobenzo[*a*]-pyrene; (E) 6-nitrobenzo[*a*]pyrene.

6-Nitrobenzo[*a*]pyrene (6-NBaP). Table 2 compares the available X-ray structural data[43] with calculations for 6-NBaP and shows excellent agreement, providing confidence in the calculations for the other two isomers. The shortest C−C bond lengths were observed experimentally for C10−C11 and C16−C15 and are also predicted by the calculations. However, these bond lengths are shorter as compared to BaP (Table 2) indicating more double bond character. The experimental C−N bond length is 1.4752 Å, whereas the calculation suggests 1.4794 Å. The C−N bond lengths follow the order 6- > 1- > 3-NBaP, reflecting more single bond character in 6-NBaP. The experimental N−O bond lengths are 1.2052 and 1.2202 Å, whereas the calculated data are 1.2244 and 1.2246 Å. The trends in N−O bond lengths follow the order 1- ∼3- > 6-NBaP. The dihedral angle between the BaP ring and the atoms O1−N2−C4−C5 and O3−N2−C4−C9 is 62.6 and 62.8°, respectively (Table 2), which are ∼8° short of the experimentally determined X-ray torsional angles of 68.5−70.6°,[43] indicative of considerable out-of-plane orientation of the nitro group relative to the aromatic plane. The ring is also planar, with the largest C−C−C−C dihedral angles predicted for C4−C5−C6−C7 and C7−C8−C9−C4 at 1.6° and the N2−C4−C5−C30 with 1.8°.

Vibrational Spectroscopy of NBaPs. Three regions of the spectrum were examined: (i) the C−H stretching (ν) (3200−2700 cm^{-1}); (ii) in-plane (δ) vibrations (1700−1000 cm^{-1}); (iii) out-of-plane (γ) vibrations (below 1000 cm^{-1}). Assignments of the observed frequencies were made by comparisons with potential energy distribution data derived from calculations at the B3LYP/6-311+G** level of theory. The detailed vibrational frequencies and comprehensive assignments of BaP and NBaPs are presented in Supporting Information Tables S10−S13.

Bands in the 3200−2700 cm^{-1} Region. The spectrum of BaP is discussed followed by the nitrated derivatives in later sections. Although bands for BaP have been reported previously, we report new bands and provide detailed potential energy distribution of the fundamental absorptions.

BaP. Figure 2A shows the IR bands for BaP (both solution and dispersed in KBr), with prominent modes at 3030 (3039), 2925 (2927), and 2856 (2855) cm^{-1}, the numbers in parentheses representing solution data. In CCl_4 solution, the bands are better resolved. The strongest Raman bands were observed at 3052, 3031, 3075, and 3013 cm^{-1} in increasing order of intensity and shown in Figure S1 (Supporting Information data). The C−H stretching modes are assigned in Table S10.

TABLE 1: Selected Experimental and Calculated Geometry Parameters of Benzo[*a*]pyrene and Nitrobenzene

	bond dists *r*(CC) (Å)				angles −C−C−C (deg)		
	calcd		expt[a]		calcd		expt[a]
param	6-31G*	6-311+G**		param	6-31G*	6-311+G**	
			BaP Molecule				
C1−C2	1.4347	1.4325	1.410	C2−C1−C6	119.8	119.8	120.1
C1−C6	1.4142	1.4129	1.418	C2−C1−C28	119.4	119.4	119.5
C5−C6	1.3835	1.3818	1.361	C1−C2−C3	119.0	119.04	118.9
C8−C9	1.3568	1.3544	1.342	C3−C2−C25	123.3	123.2	123.8
C1−C28	1.4226	1.4216	1.425	C2−C3−C14	122.6	122.53	122.4
C2−C3	1.4431	1.4411	1.436	C2−C3−C4	119.5	119.52	119.7
C3−C14	1.4319	1.4305	1.423	C4−C3−C14	117.9	117.9	118.0
C13−C14	1.3659	1.3636	1.352	C4−C11−C10	120.5	120.5	121.9
C10−C11	1.4306	1.4286	1.415	C1−C2−C25	117.7	117.8	117.3
				C6−C1−C28	120.8	120.8	120.4
				C5−C8−C9	121.5	121.5	121.3
				C8−C9−C10	121.3	121.3	121.7
			Nitrobenzene Molecule				
N2−O1	1.2307	1.2245	1.2272/1.2234[b]	O1−N2−O3	124.6	124.7	124.35/125.3[b]
C4−N2	1.4729	1.4809	1.4916/1.4862[b]	N2−C4−C5	118.8	118.8	118.3[c]
C4−C5	1.3937	1.3914	1.3911/1.399[b]	O1−N2−C4−C5	0.003	0.01	
C−H	1.0829	1.0834	1.0812/1.093[b]	C9−C4−C5−C6	0.002	0.00	
				C9−C4−C5	122.3	122.3	124.99/123.42[b]
				C−N−O	117.7	117.7	117.82/117.34[b]

[a] From ref 39 (X-ray diffraction). [b] From ref 42 (microwave/electron diffraction). [c] From ref 41 (electron diffraction).

TABLE 2: Selected C−C, C−N, and N−O Bond Lengths (Å) and C−C−N−O Dihedral Angles (deg) for BaP and 1-, 3-, and 6-Nitrobenzo[*a*]pyrene (B3LYP/6-311+G)**

		r(C−C) (Å)		*r*(C−N) (Å)		*r*(N−O) (Å)		−C−C−N−O (deg)	
PAH	param	calcd	expt	calcd	expt	calcd	expt	calcd	expt
BaP	C8−C9	1.3544	1.342[a]						
	C13−C14	1.3636	1.352[a]						
1-NBaP	C21−C22	1.3539	NA	1.4722	NA	1.2283		29.0, 27.0	NA
	C31−C32	1.3643	NA			1.2276			
3-NBaP	C21−C22	1.3549	NA	1.4732	NA	1.2280		30.5, 28.8	NA
	C26−C27	1.3631	NA			1.2275			
6-NBaP	C11−C10	1.3538	1.3413[b]	1.4794	1.4752[b]	1.2244	1.2052[b]	62.6, 62.8	68.5,[b] 70.6[b]
	C15−C16	1.3627	1.3513[b]			1.2246	1.2202[b]		

[a] From ref 39 (X-ray diffraction). [b] From ref 43 (X-ray diffraction). NA = not available.

TABLE 3: Experimental and Calculated Nitro Stretch Frequencies (cm^{-1}) for 1-, 3-, and 6-Nitrobenzo[*a*]pyrenes

nitro	ν^{asym}/expt			ν^{asym}/calcd:
PAH	IR/KBr	IR/CCl_4	Raman	6-311+G**
1-NBaP	1519	1523	1515	1532
3-NBaP	1519	1525	1518	1534
6-NBaP	1511	1528	1519	1547

nitro	ν^{sym}/expt			ν^{sym}/calcd:
PAH	IR/KBr	IR/CCl_4	Raman	6-311+G**
1-NBaP	1332	1334	1330	1324
	1310	1312	1310	1312
3-NBaP	1338	1339	1332	1329
	1318	1318	1317	1318
6-NBaP	1365	1374	1366	1361

1-NBaP. Figure 2B shows the IR spectrum of 1-NBaP in the C−H stretching region, with prominent peaks at 2919 (2927 cm^{-1} in solution) and 2855 cm^{-1}. Instead of the prominent 3030 cm^{-1} band that is observed in BaP, several weak bands are observed in this region in 1-NBaP. Detailed assignments are provided in Table S11 (Supporting Information).

3-NBaP. Figure 2C shows the IR spectrum of 3-NBaP and a profile similar to that of 1-NBaP is observed, with prominent bands at 2920 (2927) and 2851 (2854) cm^{-1} (parentheses are solution data). The bands around 3030 cm^{-1} showed considerably weaker intensities than BaP. Detailed assignments are provided in Table S12 (Supporting Information).

6-NBaP. Figure 2D shows the IR spectrum of 6-NBaP, with strong bands at 2917 (2918) and 2848 (2850) cm^{-1} (parentheses are solution data). Weak bands were observed around 3030 cm^{-1}, consistent with the other NBaPs. From a characterization point of view, the nitro compounds can be distinguished from the parent BaP by the intensity of bands in the 3000−3100 cm^{-1} range. In addition, the strong bands at ∼2854 and 2927 cm^{-1} can be used to distinguish the 1- and 3- isomers from the 6-isomer. Detailed assignments for 6-NBaP are provided in Table S13.

Bands in the 1700−1000 cm^{-1} Region. Frequencies in this region (Tables 3 and S10−S13) are mainly due to the C−H in-plane bends (δ) and C−C stretching (in the 1300−1000 cm^{-1} region) motions coupled with the ring C−C−H bending modes, as well as the symmetric and asymmetric nitro stretches.

BaP. Figure 3 compares the calculated, solid, and solution spectra of BaP. Figure 7A shows the Raman spectrum. The agreement between theory and experimental IR data for BaP is remarkable and, on average, within 5 cm^{-1}. Although frequencies of BaP have been reported,[16−19,44] no comprehensive assignments have been made. Table S10 (Supporting Information) lists the assignments of the major BaP peaks. Comparisons between Raman and IR spectra provide interesting information.

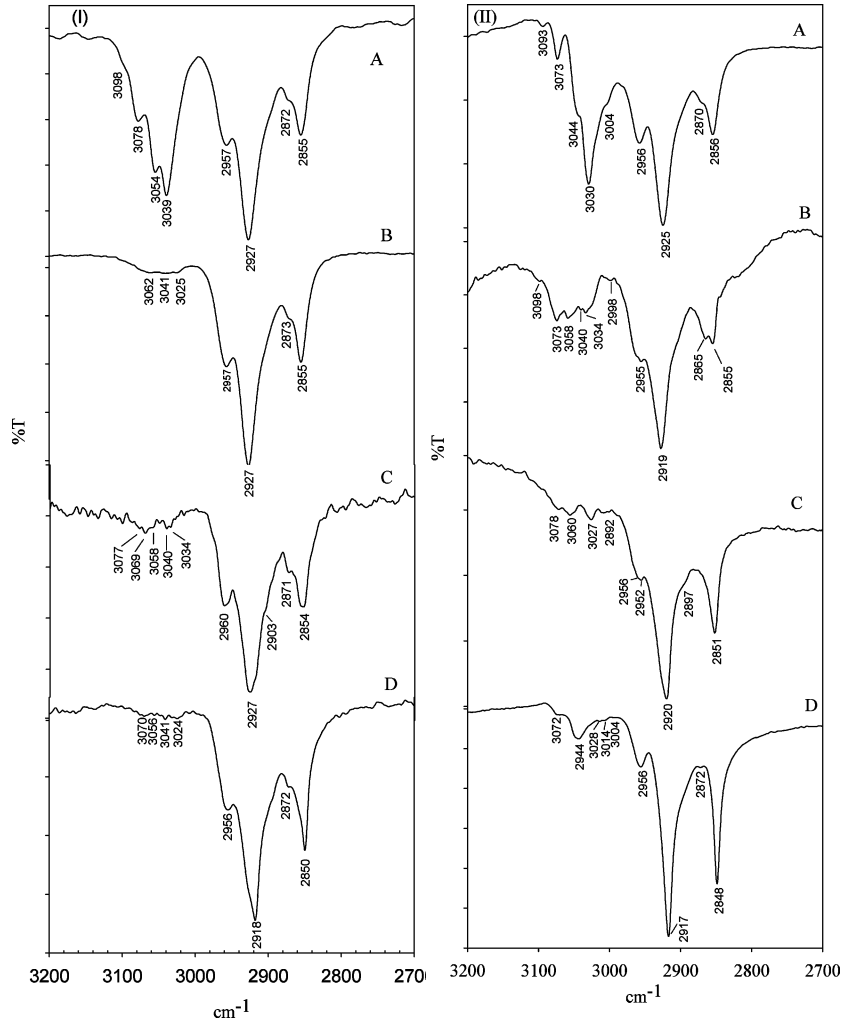

Figure 2. FT-IR spectra in the 3200−2700 cm^{-1} region in solution (panel I, left, CCl_4) and solid phases (panel II, right, KBr pellet): (A) BaP; (B−D) 1-, 3-, and 6-NBaP (4 cm^{-1} resolution).

The bands at 1387 and 1236 cm^{-1} showed strong intensities in Raman in contrast to the IR. Both bands are characterized by ring stretching motions, with the 1236 cm^{-1} band also having contributions from δ(C−H) displacements. The prominent bands in the IR (solution) at 1181, 1244, 1270, 1314, 1409, 1416, 1460, 1466, and 1620 cm^{-1} all have significant contributions from ring stretching and δ(C−H) bending motions.

1-NBaP. The IR data in KBr and CCl_4 solution along with the calculated spectra are shown in Figure 4, with the detailed assignments in Table S11 (Supporting Information). The simulated frequencies are in good agreement with experimental bands, with average deviations of <5 cm^{-1}. The Raman spectrum is shown in Figure 7B. The nitro group vibrations were identified on the basis of comparisons between 1-NBaP and BaP, as well as examining the potential energy distributions. For the asymmetric (ν_{asNO_2}) NO_2 stretch, the calculations predict that bands at 1512, 1532, 1567, and 1580 cm^{-1} all have NO_2 motion, with the largest contribution for the 1532 cm^{-1} band. Figure 8A shows the normal mode corresponding to the 1532 cm^{-1} band. The corresponding experimental band in the solid IR is at 1519 cm^{-1} and in solution at 1523 cm^{-1}. In contrast to the IR band, the ν_{asNO_2} Raman band, assigned at 1515 cm^{-1}, is very weak. Contributions to the symmetric nitro motion were found for bands calculated at 1312, 1324, and 1347 cm^{-1}, with major contributions to the 1312 and 1324 cm^{-1} band, the normal modes corresponding to which are shown in Figure 8A. The observed IR frequencies are at 1310 and 1332 cm^{-1} for the solid and 1312 and 1334 cm^{-1} in solution, with the corresponding Raman bands at 1310 and 1330 cm^{-1}. The bands at 1627, 1618, 1594, 1581, 1565, and 1540 cm^{-1} (all IR solid state, but with corresponding bands in solution and Raman) are assigned to ν(CC) and δ(CH). The Raman spectrum also shows a strong band at 1241 cm^{-1}.

3-NBaP. Figure 5 shows the IR spectra of 3-NBaP in the solid state and solution along with the calculated spectra. Figure 7C shows the Raman spectrum. The calculated frequencies are in fairly good agreement with the IR data with average deviations of <5 cm^{-1}, and detailed assignments of all observed bands are presented in Table S12 (Supporting Information). The overall appearances of the IR and Raman spectra are similar to those of 1-NBaP. The potential energy distributions suggest that bands at 1568, 1534, and 1511 cm^{-1} have contributions from the asymmetric nitro group vibration, with the prominent band being at 1534 cm^{-1}, the normal mode for which is shown in Figure 8B. The ν_{asNO_2} IR band is at 1519 cm^{-1} in the solid state and 1525 cm^{-1} in solution. The corresponding Raman band at 1518 cm^{-1} is very weak. The calculated vibrational modes corresponding to ν_{sNO_2} are predicted at 1329 and 1318 cm^{-1}, with minor contribution also to the 1308 cm^{-1} band. The corresponding experimental bands in the IR are at 1338, 1318, and 1310 cm^{-1} (solid) and 1338, 1319, and 1311 cm^{-1} (solution), whereas, in the Raman, bands appear at 1332, 1317, and 1310 cm^{-1}. The normal modes corresponding to ν_{sNO_2} are shown in Figure 8B. The prominent bands in the Raman

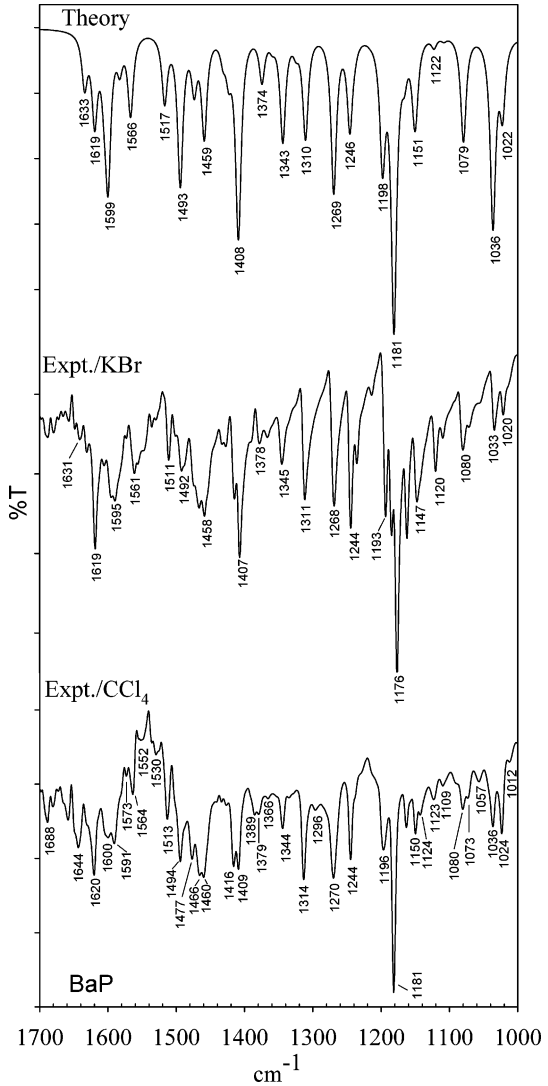

Figure 3. FT-IR and calculated IR spectra of benzo[*a*]pyrene (BaP, B3LYP/6-311+G** level of theory) in the 1700−1000 cm^{-1} region (resolution 4 cm^{-1}, KBr, CCl_4).

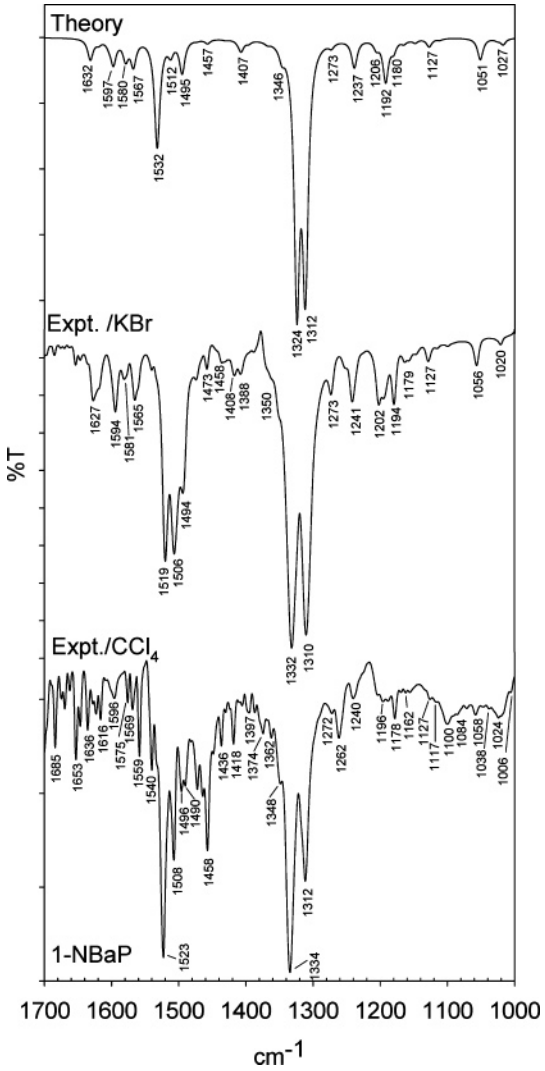

Figure 4. FT-IR and calculated IR spectra of 1-nitrobenzo[*a*]pyrene (1-NBaP, B3LYP/6-311+G** level of theory) in the 1700−1000 cm^{-1} region (resolution 4 cm^{-1}, KBr, CCl_4).

spectrum (Figure 7C) are assigned as follows: Bands at 1623, 1615, and 1585 cm^{-1} are due to the δ(CH) coupled to the ν(CC). The most pronounced band at 1386 cm^{-1} is assigned to δ(CH) coupled to ν(CC), while the 1224 and 1184 cm^{-1} bands are δ(CH) bands. The aromatic in-plane C−H bending modes (δ(CH)) coupled to the ν(CC) vibrations are expected in the 1250−1000 cm^{-1} region.

6-NBaP. The IR and Raman spectra of 6-NBaP in the 1700−1000 cm^{-1} region are shown in Figures 6 and 7D. Vibrational data for 6-NBaP have been reported,[8] and assignments based on group tables have been made. The present studies provide more detailed vibrational assignments and are presented in Table S13 (Supporting Information). In the ν_{asNO_2} region, the calculations predict that the band at 1547 cm^{-1} is primarily a nitro asymmetric stretching mode, with the normal mode shown in Figure 8C. The band at 1565 cm^{-1} also has minor contributions from the asymmetric motion. The primary ν_{asNO_2} band observed in the IR is at 1511 cm^{-1}, while, in solution, the band appears at 1528 cm^{-1}. The Raman spectrum shows a weak band at 1519 cm^{-1}. Calculations suggest that ν_{sNO_2} is at 1361 cm^{-1}, and on the basis of the new bands that show up after 6-NO_2 substitution, we assign bands at 1365 cm^{-1} to the symmetric NO_2 stretch (solution 1374 cm^{-1}). The normal mode corresponding to this vibration is shown in Figure 8C. Unlike 1- and 3-NBaP, the Raman spectrum of 6-NBaP shows no prominent band due to the ν_{sNO_2} stretch; a very weak band is observed at 1366 cm^{-1}. The band at 1384 cm^{-1} in the IR (Raman 1383 cm^{-1}) was previously assigned to a nitro group vibration.[8] We assign it to δ(C−H) on the C10−C11 positions coupled to ring ν(CC) stretches (calculation 1372 cm^{-1}). The band at 1326 cm^{-1} has also been assigned to the ν_{sNO_2} stretch,[8] but calculations suggest that it is a mode involving C−C stretch (ring).

There is marked similarity between the $\nu_{s/asNO_2}$ stretches for 1- and 3-BaP. The C−C−N−O dihedral angle, i.e., orientation of the NO_2 group relative to the plane of the BaP ring, is similar in the 1- and 3-NBaP isomers (∼29°) as compared to the more out-of-plane orientation (62°) in 6-NBaP. With increased twisting, there will be reduced $\pi-\pi$ interactions between the nitro group and the ring, leading to an elongated C−N bond and a reduced N−O bond length in 6-NBaP. This is reflected in the calculated C−N bond lengths, with 6-NBaP having the longest C−N bond by 0.006 Å (Table 2). Indeed, the C−N bond length is shortest for the smallest calculated dihedral angle for the C−C−N−O nitro orientation. The asymmetric and especially the symmetric stretching vibrations of 6-NBaP occur at higher frequencies than the other two isomers.

Bands in the 1000−450 cm^{-1} Region. In general, bands below 1000 cm^{-1} are mainly characterized as out-of-plane C−H

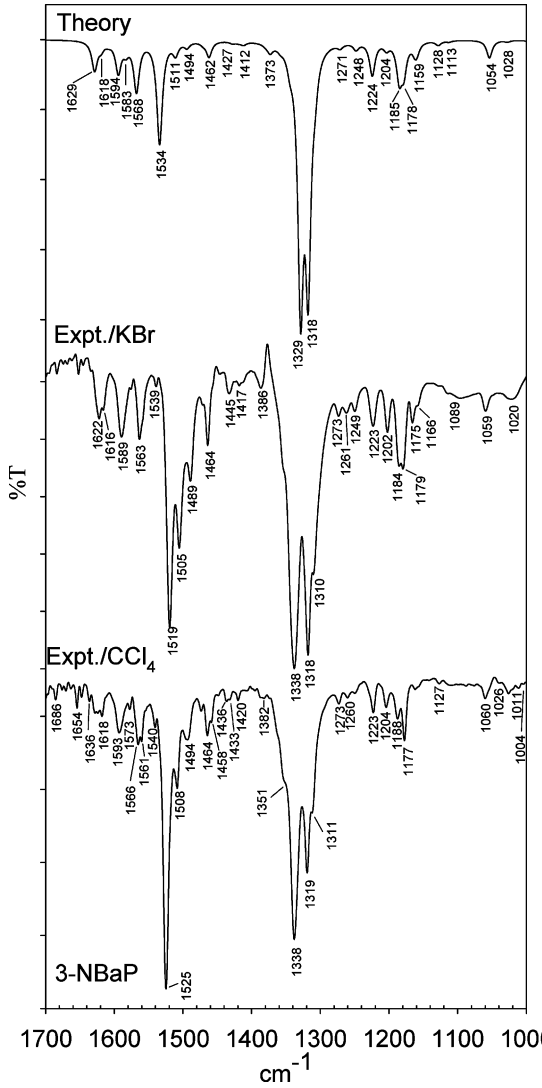

Figure 5. FT-IR and calculated IR spectra of 3-nitrobenzo[*a*]pyrene (3-NBaP, B3LYP/6-311+G** level of theory) in the 1700−1000 cm^{-1} region (resolution 4 cm^{-1}, KBr, CCl_4).

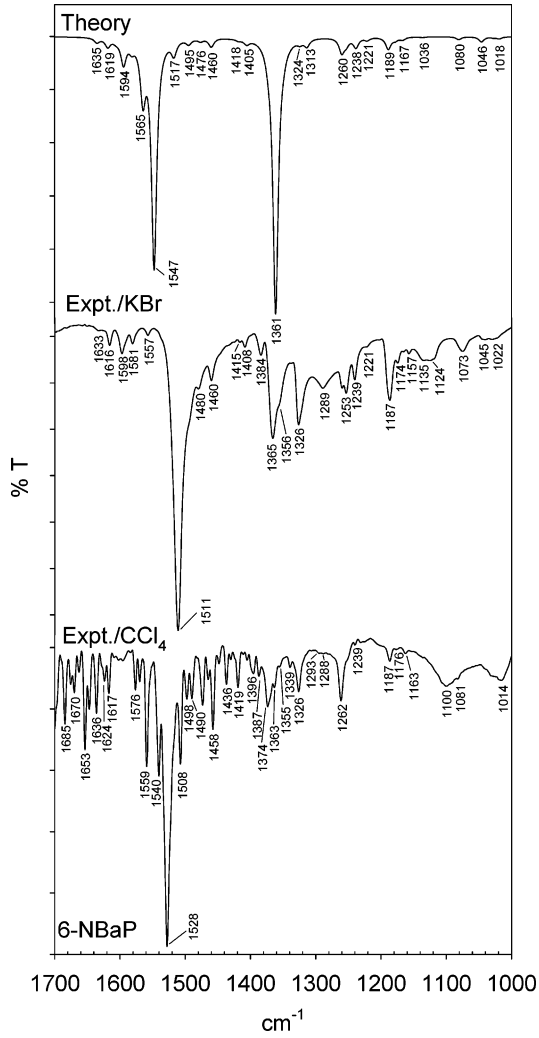

Figure 6. FT-IR and calculated IR spectra of 6-nitrobenzo[*a*]pyrene (6-NBaP, B3LYP/6-311+G** level of theory) in the 1700−1000 cm^{-1} region (resolution 4 cm^{-1}, KBr, CCl_4).

bends (γ(CH)).[45] Ring deformations mainly occur below 450 cm^{-1}.[46] The IR and Raman data are shown in Figures S2 and S3 in the Supporting Information. The computed spectra are in very good agreement with the experimental data.

BaP. The bands at 756, 762, and 802 cm^{-1} are characterized as C−C ring torsions (τ(CC)). Bands at 668, 634, 561, 534, 526, 510, 494, and 455 cm^{-1} are mixed torsions and γ(C−H) bends.

1-NBaP. The strongest IR bands were measured at 890, 880, 855, 845, 822, 806, 780, 752, and 686 cm^{-1}, with the bands at 752, 780, and 880 cm^{-1} involving NO_2 motions. The strong Raman bands at 647, 778, and 808 cm^{-1} are assigned to in-plane bends involving the ring and NO_2 groups.

3-NBaP. Bands involving nitro group distortions occur at 713, 759, 829, 869, and 940 cm^{-1}. Strong Raman bands at 870, 810, 650, 638, and 530 cm^{-1} are mainly γ(CH) bands.

6-NBaP. Comparison of 6-NBaP with that of BaP showed new peaks appearing at 652, 786, and 859 cm^{-1}, with the latter two bands involving nitro group motion.

Bands below 450 cm^{-1}. IR spectra could not be obtained below 450 cm^{-1}.[46] Raman frequencies were matched with calculated frequencies, and their assignments were made in Tables S10−S13. The data are shown in Figure S4 in the Supporting Information.

Discussion

Perturbation of the Ring upon Nitro Group Substitution. Substitution of the NO_2 group on the BaP framework leads to major structural changes, primarily due to the steric interaction of the oxygens of the nitro group with the peri hydrogens. Starting with the optimized geometries of the three nitro isomers, the NO_2 group was brought into the plane of the aromatic ring (CCNO angle = 180°), and the distances from the oxygen to the peri hydrogens in the same plane were determined. For 1-NBaP, the distances are 1.96 and 2.29 Å and, for 3-NBaP, 1.93 and 2.29 Å, whereas, for 6-NBaP, the distances are 1.69 and 1.70 Å. To ease the steric repulsion with the peri hydrogens, the geometric adjustments in the three isomers are quite different. For 1- and 3-NBaP, the ring at which the substitution occurs distorts slightly (as evidenced by the N2C4C5C32 angle of 3° for 1-NBaP and N2C4C5C22 angle of 2.7° for 3-NBaP) and the NO_2 group also rotates out of plane by ∼29°. However, for the 6-NBaP, the ring distortion is considerably smaller (N2C4C5C30 angle of 1.8°) and the NO_2 group is rotated by about 62.8° (68.5−70.6° from crystal data).[43] There are two structural aspects which are evident from these geometries. First, there is more flexibility of the ring at which the 1- and 3-substitutions take place. Second, because of the lack of flexibility of the ring, the nitro group at the 6-position has to undergo a significantly larger rotation out-of-plane to avoid the

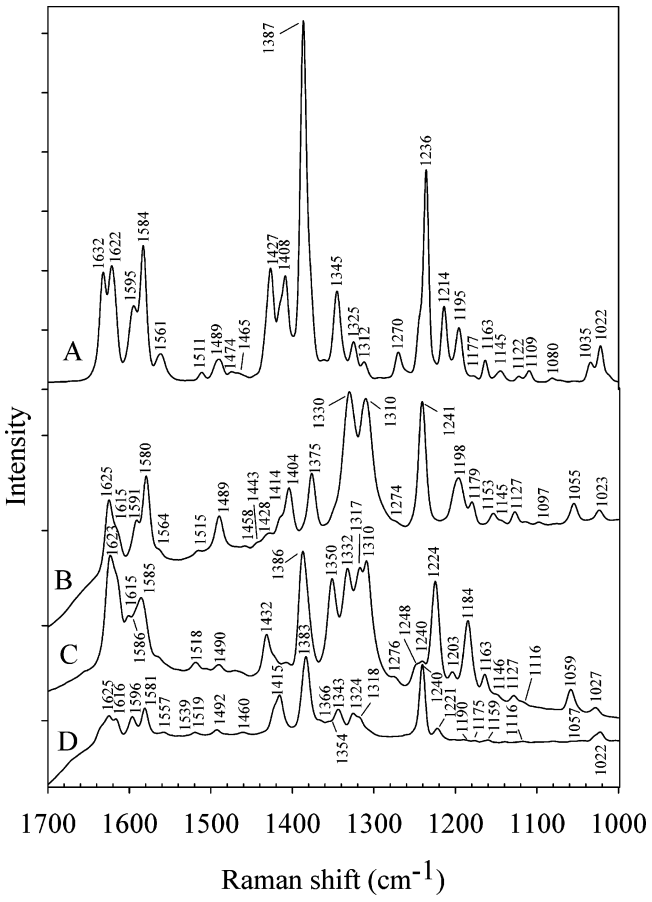

Figure 7. FT-Raman of (A) benzo[*a*]pyrene (BaP), (B) 1-NBaP, (C) 3-NBaP, and (D) 6-NBaP. Spectra were acquired at 4 cm^{-1} resolution in a KBr pellet.

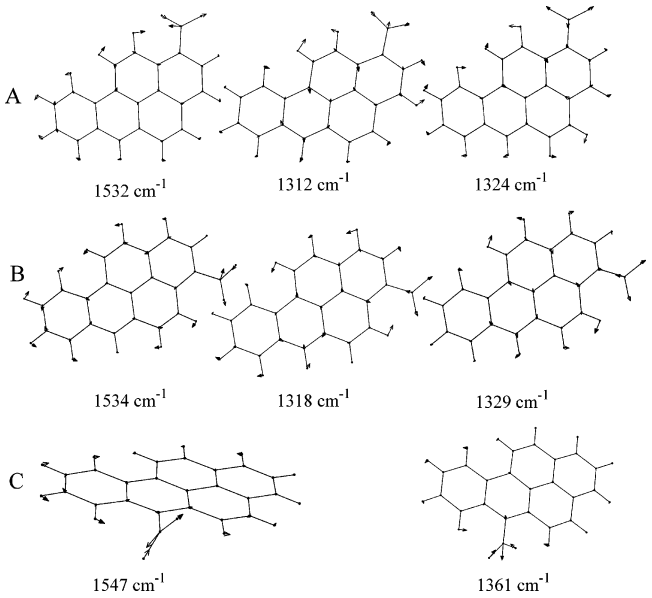

Figure 8. Normal modes corresponding to the asymmetric and symmetric nitro stretches of (A) 1-, (B) 3-, and (C) 6-nitrobenzo[*a*]-pyrenes.

shorter O···H distances. Correlation between photocleavage of the NO_2 group and its orientation has been proposed;[47] e.g., for 9-nitroanthracene (9-NA), the C−C−N−O dihedral angle is 85° relative to the aromatic moiety and it is degraded faster as compared to 1-nitroanthracene (1-NA) on exposure to radiation.[48] On the basis of this correlation, the photodegradation of NBaPs should follow the order 6-NBaP > 1- ≈ 3-NBaP.

Nitro Group Vibrations. The frequencies of the asymmetric and symmetric nitro vibrations increase as the NO_2 group rotates out of plane (especially evident in the IR spectra). This is particularly true for the symmetric stretch in the IR which varies from 1365 cm^{-1} in case of 6-NBaP to 1332−1310 and 1338−1318 cm^{-1} in case of 1- and 3-NBaP, respectively. These trends can be correlated with the lengthening of the C−N bond and shortening of the N−O bond as the NO_2 group rotates out of plane of the BaP ring (Tables 2 and 3).

The only other nitroPAH for which detailed vibrational studies, including calculations, have been reported is 1-nitropyrene (1-NPy),[23,24] and a comparison with the present study of NBaP provides insight into the vibrational spectroscopy of these compounds. Geometry optimization of 1-NPy suggests that the NO_2 group is 32° out of the plane of the aromatic ring and is thus similar to 1- and 3-NBaP. The symmetric stretches of the nitro group of 1-NPy appear at ∼1310 and 1330 cm^{-1} and the asymmetric stretch appears at ∼1507 cm^{-1}, which compare very well with the data in Table 3 for 1- and 3-NBaP. The intensity profile in the nitro group stretching region of 1-NPy is also similar to that of the 1- and 3-NBaP isomers. However, the vibrational profile of 6-NBaP is quite distinct; the intensity of the symmetric nitro stretch in both the IR and Raman is very weak. It is unclear at this point if this pattern is related to the fact that the NO_2 group is significantly out-of-plane in the 6-NBaP isomer (62°), and only with detailed vibrational data on other nitropolycyclic aromatic hydrocarbons can the validity of these trends be established.

Biological Activity of N-BaPs. Nitrated BaPs exhibit different mutagenic properties against bacterial and mammalian cells.[5,7,27,49] The mutagenic activities of 1-, 3-, and 6-NBaP against TA98 *S. typhimurium* (without an S9 microsomal treatment) were determined as 830, 2400, and 0 rev/(nmol/plate), respectively. In the same study, 1- and 3-NBaP each produced the same biological activities against the TA98NR (a nitroreductase-deficient strain). It has been suggested that the orientation of the nitro group relative to the BaP aromatic ring is an important structural feature that may be predictive of observed mutagenic effects.[8] The hypothesis is that the C−C−N−O dihedral angle determines the extent to which the NBaPs lock into the nitroreductase enzymes during reduction. The more planar orientation of the 1- and 3-NBaP favors the binding to the nitroreductase enzyme, as well as presence of the peri hydrogens at the 5- and 7-positions in 6-NBaP impedes the access of the molecule to the enzyme.

Conclusions

The isomeric 1-, 3-, and 6-nitrobenzo[*a*]pyrenes were synthesized, and their IR and Raman spectra were recorded. DFT calculations at the B3LYP/6-311+G** level of theory were used to calculate the geometry of the parent PAH and the nitro isomers, as well as to predict the vibrational spectra. Good agreement between the calculated and known crystal structures of nitrobenzene and benzo[*a*]pyrene provided confidence in the calculations. Complete vibrational assignments were made from potential energy distributions for the nitrated benzo[*a*]pyrenes, with particular emphasis on the nitro group vibrations. On the basis of these results, correlations between the vibrational spectra and structural parameters such as C−C−N−O dihedral angles and the C−N and N−O bond lengths have been made. In addition, correlations between the biological activity of the N-BaPs and structural features are indicated.

Acknowledgment. We acknowledge financial support from the Ohio State Environmental Molecular Science Institute,

funded by the National Science Foundation (Grant CHE-0089147, EMSI program), and the Ohio Supercomputer Center for generous allocations of computer time. We thank Professor Leo Paquette for the use of the MPLC equipment, Professor Siva Umapathy for the NMODES program as well as John Merle for useful discussions. K.K.O. thanks the Lubrizol Co. for a fellowship.

Supporting Information Available: Optimized geometries at the B3LYP/6-311+G** level (Tables S1−S9), experimental and theoretical vibrational spectroscopic data with PEDs (Tables S10−S13), and Figures S1−S4, showing Raman and IR spectra in the C−H stretching region as well as vibrations below 1000 cm^{-1}. This material is available free of charge via the Internet at http://pubs.acs.org.

References and Notes

(1) Arey, J.; Zielinska, B.; Atkinson, R.; Aschmann, S. M. *Int. J. Chem. Kinet.* **1989**, *21*, 775.

(2) Pitts, J. N., Jr.; Lokensgard, D. M.; Ripley, P. S.; van Cauwenberghe, K. A.; van Vaeck, L.; Shaffer, S. D.; Thill, A. J.; Belser, W. L. *Science* **1980**, *210*, 1347.

(3) Jager, J. *J. Chromatogr.* **1978**, *152*, 575.

(4) Ishii, S.; Hisamatsu, Y.; Inazu, K.; Kobayashi, T.; Aika, K. *Chemosphere* **2000**, *41*, 1809.

(5) Fukuhara, K.; Kurihara, M.; Miyata, N. *J. Am. Chem. Soc.* **2001**, *123*, 8662.

(6) Fukuhara, K.; Miyata, N.; Matsui, M.; Matsui, K.; Motoi, I. J.; Kamiya, S. *Chem. Pharm. Bull.* **1990**, *38*, 3158.

(7) Chou, M. W.; Heflich, R. H.; Casciano, D. A.; Miller, D. W.; Freeman, J. E.; Evans, F. E.; Fu, P. P. *J. Med. Chem.* **1984**, *27*, 1156.

(8) Li, Y. S.; Fu, P. P.; Church, J. S. *J. Mol. Struct.* **2000**, *550*−*551*, 217.

(9) Hudgins, D. M.; Sandford, S. A. *J. Phys. Chem A* **1998**, *102*, 353.

(10) Hudgins, D. M.; Sandford, S. A. *J. Phys. Chem. A* **1998**, *102*, 344.

(11) Hudgins, D. M.; Bauschlicher, C. W., Jr.; Allamandola, L. J. *Spectrochim. Acta, Part A* **2001**, *57*, 907.

(12) Langhoff, S. R. *J. Phys. Chem.* **1996**, *100*, 2819.

(13) Langhoff, S. R.; Bauschlicher, C. W., Jr.; Hudgins, D. M.; Sandford, S. A.; Allamandola, L. J. *J. Phys. Chem. A* **1998**, *102*, 1632.

(14) Onchoke, K. K.; Hadad, C. M.; Dutta, P. K. *Polycyclic Aromat. Compd.* **2004**, *24*, 37.

(15) Visser, T.; Vredenbregt, M. J.; de Long, A. P. J. M. *J. Chromatogr., A* **1994**, *687*, 303.

(16) Goodpaster, J. V.; Harrison, J. F.; McGuffin, V. L. *J. Phys. Chem. A* **1998**, *102*, 3372.

(17) Semmler, J.; Yang, P. W.; Crawford, G. E. *Vib. Spectrosc.* **1991**, *2*, 189.

(18) Colangeli, L.; Mennella, V.; Barata, G. A.; Bussoletti, E.; Strazzulla, G. *Astrophys. J.* **1992**, *396*, 369.

(19) Chiang, H.-P.; Mou, B.; Li, K. P.; Chiang, P.; Wang, D.; Lin, S. J.; Tse, W. S. *J. Raman Spectrosc.* **2001**, *32*, 45.

(20) Gittins, C. M.; Rohlfing, E. A.; Rohlfing, C. M. *J. Chem. Phys.* **1996**, *105*, 7323.

(21) Juchnoviski, I. N.; Andreev, G. N. *Acad. Bulg. Sci.* **1976**, *29*, 1637.

(22) Juchnovski, I. N.; Andreev, G. N. *Bulg. Acad. Sci.* **1983**, *16*, 389.

(23) Carrasco F, E. A.; Campos-Vallette, M. M.; Leyton, P.; Diaz, F. G.; Clavijo, R. E.; Garcia-Ramos, J. V.; Inostroza, N.; Domingo, C.; Sanchez-Cortes, S.; Koch, R. *J. Phys. Chem. A* **2003**, *107*, 9611.

(24) Carrasco-Flores, E. A.; Clavijo, R. E.; Campos-Vallette, M. M.; Aroca, R. F. *Appl. Spectrosc.* **2004**, *58*, 555.

(25) Dyker, G.; Kadzimirsz, D.; Thörne, A. *Eur. J. Org. Chem.* **2003**, *2003*, 3162.

(26) Dewar, M. J. S.; Mole, T.; Urch, D. S.; Warford, E. W. T. *J. Chem. Soc. (London)* **1956**, 3572.

(27) Pitts Jr, J. N.; Zielinska, B.; Harger, W. P. *Mut. Res.* **1984**, *140*, 81.

(28) Johansen, E.; Sydes, L. K.; Greibrokk, T. *Acta Chem. Scand.* **1984**, *B38*, 309.

(29) Frisch, M. J.; Trucks, G. W.; Schlegel, H. B.; Scuseria, G. E.; Robb, M. A.; Cheeseman, J. R.; Zakrzewski, V. G.; Montgomery Jr., J. A.; Stratmann, R. E.; Burant, J. C.; Dapprich, S.; Millam, J. M.; Daniels, A. D.; Kudin, K. N.; Strain, M. C.; Farkas, O.; Tomasi, J.; Barone, V.; Cossi, M.; Cammi, R.; Mennucci, B.; Pomelli, C.; Adamo, C.; Clifford, S.; Ochterski, J.; Petersson, G. A.; Ayala, P. Y.; Cui, Q.; Morokuma, K.; Malick, D. K.; Rabuck, A. D.; Raghavachari, K.; Foresman, J. B.; Cioslowski, J.; Ortiz, J. V.; Stefanov, B. B.; Liu, G.; Liashenko, A.; Piskorz, P.; Komaromi, I.; Gomperts, R.; Martin, R. L.; Fox, D. J.; Keith, T.; Al-Laham, M. A.; Peng, C. Y.; Nanayakkara, A.; Gonzalez, C.; Challacombe, M.; Gill, P. M. W.; Johnson, B.; Chen, W.; Wong, M. W.; Andres, J. L.; Gonzalez, C.; Head-Gordon, M.; Replogle, E. S.; Pople, J. A. *Gaussian 98*, revision A.9; Gaussian, Inc.: Pittsburgh, PA, 1998.

(30) Becke, A. D. *J. Chem. Phys.* **1983**, *98*, 5643.

(31) Becke, A. D. *Phys. Rev. A* **1988**, *38*, 3098.

(32) Lee, C.; Yang, W.; Parr, R. G. *Phys. Rev. B* **1988**, *37*, 785.

(33) Hariharan, P. C.; Pople, J. A. *Theor. Chim. Acta* **1973**, *28*, 213.

(34) Scott, A. P.; Radom, L. *J. Phys. Chem.* **1996**, *100*, 16502.

(35) Banisaukas, J.; Szczepanski, J.; Vala, M.; Hirata, S. *J. Phys. Chem. A* **2004**, *108*, 3713.

(36) Lee, S. Y. *J. Phys. Chem. A* **2001**, *105*, 8093.

(37) Mohandas, P.; Umapathy, S. *J. Phys. Chem. A* **1997**, *101*, 4449.

(38) Portmann, S.; Lüthi, H. P. *CHIMIA* **2000**, *54*, 766.

(39) Iball, J.; Scrimgeor, S. N.; Young, D. W. *Acta Crystallogr.* **1976**, *B32*, 328.

(40) Irle, S.; Krygowski, T. M.; Niu, J. E.; Schwarz, H. E. *J. Org. Chem.* **1995**, *60*, 6744.

(41) Shishkov, I. F.; Sadova, N. I.; Novikov, V. P.; Vilkov, L. V. *J. Struct. Chem. (Zh. Strukt. Khim.)* **1984**, *25*, 260.

(42) Domenicano, A.; Schultz, G.; Hargittai, I.; Colapietro, M.; Portalone, G.; George, P.; Bock, C. W. *Struct. Chem.* **1990**, *1*, 107.

(43) Warner, S. D.; Lebuis, A.-M.; Farant, J.-P.; Butler, I. S. *J. Chem. Crystallogr.* **2003**, *33*, 213.

(44) Stewart, S. D.; Fredericks, P. M. *J. Raman Spectrosc.* **1995**, *26*, 629.

(45) Mamantov, G.; Garrison, A. A.; Wehry, E. L. *Appl. Spectrosc.* **1982**, *36*, 339.

(46) Langley, C. H.; Lii, J.-H.; Allinger, N. L. *J. Comput. Chem.* **2001**, *22*, 1426.

(47) Fu, P. P.; Tungeln, L. S. V.; Chou, M. W. *Carcinogenesis* **1985**, *6*, 753.

(48) Warner, S. D.; Farrant, J.-P.; Butler, I. S. *Chemosphere* **2004**, *54*, 1207.

(49) Tungeln, L. S.; Xia, Q.; Bucci, T.; Heflich, R. H.; Fu, P. P. *Cancer Lett.* **1999**, *137*, 137.